Crystalline and electronic structure of Pu–Ce and Pu–Ce–Ga alloys stabilized in the δ phase

Marion Dormeval, Nathalie Baclet, C. Valot, P. Rofidal, Jean Marc Fournier

Crystalline and electronic structure of Pu–Ce and Pu–Ce–Ga alloys stabilized in the δ phase

M. Dormeval[a,*], N. Baclet[a], C. Valot[a], P. Rofidal[a], J.M. Fournier[b]

[a]*CEA-Centre de Valduc, 21120 Is sur Tille, France*
[b]*Université Joseph Fourier LEG-INPG, BP 46, 38402 Saint Martin d'Hères Cedex, France*

In the actinides series (which corresponds to the progressive filling of the 5f sub-shell), plutonium lies at the changeover for the behavior of the 5f electrons between the light actinides (up to Np) with delocalized 5f states, and the heavy actinides (from Am on) with localized 5f states. At this boundary, the expanded δ-phase exhibits an intermediate and thus controversial behavior of its 5f electrons. This high temperature δ-phase can be stabilized at and below room temperature by alloying with so-called deltagen solutes Ga, Al, Ce and Am. In this work, some Pu–Ce and Pu–Ce–Ga alloys were studied using several techniques (dilatometry, X-ray diffraction (XRD), extended X-ray absorption fine structure spectroscopy (EXAFS), electrical resistivity and magnetic susceptibility). It is found that the mechanism of δ-Pu stabilization is far from straightforward as both Pu 5f and Ce 4f electronic states are involved, inducing complex crystalline organization while no clear localization of the 5f states can be deduced from experimental results. Ternary Pu–Ce–Ga alloys show cooperative deltagen effects of Ce and Ga.

Keywords: Actinide alloys; EXAFS; X-ray diffraction; Magnetic measurements

1. Introduction

In the actinides series, corresponding to the progressive filling of the 5f sub-shell, plutonium (Pu) lies at the crossover between two sub-families, the light and the heavy actinides: the light actinides (from protactinium (Pa) to neptunium (Np)) in which the 5f electrons are bonding and exhibit a band character similar to that of d electrons in transition metals, and the heavy actinides (from americium (Am) to lawrencium (Lw)) with localized, non-bonding, 5f electrons comparable to the 4f electrons in the lanthanide series. Moreover, this transition from delocalization to localization of the 5f electrons in the actinides takes place within the plutonium phase diagram, following its numerous allotropic changes (α, β, γ, δ, δ′, ε) and the associated volume changes, focusing on the α–δ transition.

At room temperature, plutonium is monoclinic (α-Pu) and most people now agree that the 5f electron states, although correlated, are itinerant in this phase. Between 592 and 730 K, plutonium is face-centered-cubic (f.c.c. δ-Pu) and various experimental and theoretical approaches [1,2], corroborate the straightforward volume information: δ-Pu is intermediate between α-Pu and Am and so is the behavior of its 5f electrons. While theoretical studies can be performed without any problem on pure δ-Pu even at $T=0$, experimentally, it is necessary to chemically stabilize this high temperature phase at and below room temperature by alloying in order to investigate this allotrope using usual techniques. In doing so, the true structure of pure δ-Pu is perturbed and one is then obliged to study the behavior of the alloys as a function of composition in order to obtain the behavior of pure δ-Pu by extrapolation. On the other hand, these studies in themselves may help to better understand the stabilization mechanisms and thus the electronic structure of pure δ-Pu.

Only four such deltagen elements exist leading to substitutional solid solutions of δ-stabilized Pu alloys at and below room temperature: gallium (Ga), aluminum (Al), cerium (Ce) and americium (Am). The case of scandium (Sc) is more controversial since for both Ellinger et al. [3] and Kutaitsev et al. [4] the phase diagram at room temperature remains uncertain.

While Ga and Al atoms are smaller than δ-Pu, Ce and

*Corresponding author.
E-mail address: marion.dormeval@cea.fr (M. Dormeval).

Am are larger so that a priori the size of dopant does not seem to be the primary control parameter. Ga and Al atoms (r_{Ga}=1.41 Å[1], r_{Al}=1.43 Å) are respectively 14 and 13% smaller than δ-Pu atoms ($r_{\delta\text{-Pu}}$=1.64 Å). They stabilize the δ-phase for Ga and Al contents ranging from 0.8 to 10 at.% and 2.5 to 10 at.%, respectively. X-ray diffraction (XRD) studies performed on different Pu–Ga [8] and Pu–Al [9] alloys show not only a decrease in the lattice parameter but even a negative deviation from Vegard's law with increasing Ga and Al contents. Extended X-ray absorption fine structure spectroscopy (EXAFS) investigations of Pu–Ga alloys [10,11], have shown Ga to be substitutional with an almost 4% shrinkage of the nearest plutonium atoms towards the Ga atoms. According to the authors, this contraction suggests hybridization between Ga 4p electronic states and plutonium 5f electronic states which explains the decrease in the δ-Pu radius resulting in the observed negative deviation from Vegard's law.

This approach is corroborated by theoretical calculations [12], unpublished calculations by Eriksson and Boring, cited by Cox et al. [11]. Thus one could surprisingly conclude that Ga (Al) atoms stabilize the δ phase through 4p (3p)–5f hybridization, i.e. 5f electron states delocalization, more precisely by replacing 6d–5f hybridization by 4p (3p)–5f hybridization when substituting Pu by Ga (Al). This mechanism for δ-phase stabilization is in agreement with more recent theories [13] in which the broadening of the 5f bands favors higher symmetry crystal structures.

Another possibility could be hybridization between the ligand 4p(3p) electron states and Pu 6d electron states, which would then reduce the 5f–6d hybridization and then leave the 5f states more localized [14]. However, no such localization is experimentally observed by, e.g. magnetic susceptibility measurements.

Ce and Am atoms ($r_{\alpha\text{-Ce}}$=1.71 Å, $r_{\gamma\text{-Ce}}$=1.82 Å, $r_{\beta\text{-Am}}$= 1.73 Å) are respectively 4, 11 and 5.5% larger than δ-Pu atoms. Am stabilizes δ-Pu for contents ranging from 5 to 76 at.%. Ce stabilizes δ-Pu for contents ranging from 4.5 to 17 at.%. Between 17 at.% and 75 at.% Ce, the solid solution can be quenched at room temperature and is again stable between 75 and 100 at.% of Ce [15].

Both Pu–Ce and Pu–Am alloys have been much less studied than Pu–Al or Pu–Ga alloys. Handling of Pu–Am alloys presents obvious difficulties due to the high radioactivity of Am. Results on Pu–Am will be presented in forthcoming papers but preliminary XPS measurements [16] showed effectively a localization of the 5f electron states for americium contents higher than 25 at.%.

This work describes the behavior of Ce regarding the stability of δ-Pu as studied both from a crystalline structure point of view (thermal expansion, XRD, EXAFS) and an electronic structure point of view (electrical resistivity, magnetic susceptibility).

[1]Radii are calculated using a coordination number of twelve for gallium [5], aluminum [5], americium [6], and cerium [7].

The Pu–Ce alloys are all the more interesting because Ce and Pu exhibit very related electronic properties linked to the anomalous character of the f states: both 4f states in Ce and 5f states in Pu are at the threshold of localization. Thus, in δ-Pu–Ce alloys, Ce can be in the γ-Ce form or in the α-Ce form depending on the composition. Moreover, since two different mechanisms (f–p hybridization and f localization) both lead to the stabilization of the δ-Pu phase, ternary Pu–Ce–Ga alloys were also studied in order to determine if Ga and Ce had an antagonist or a cooperative effect when both present. Experimental details are described in Section 2. Results are given in Section 3 and discussed from crystalline and electronic structures's points of views in Section 4 before concluding.

2. Experimental details

2.1. Samples

Four binary Pu–Ce alloys and two ternary Pu–Ce–Ga alloys were synthesized. Alloys were made from solid or powdery Ce (99.9 wt.%), and solid Ga (99.99 wt.%) and Pu pieces. Weightings of Pu (500 g), Ce (from 3 to 33 g) and, for the ternary alloys, Ga (1.3 g), were placed in tantalum crucibles and induction melted at 1373 K for 2 h. The mixtures were then casted into graphite moulds at 773 K and cooled down to room temperature. After the machining of the ingots into samples of required geometry, a heat treatment at 733 K for 200 h under high vacuum was performed to homogenize the solute concentrations. Chemical analyses are displayed in Table 1. Results are given in atomic percent, as in all the following.

2.2. Experimental set-up

The thermal expansion experiments were performed in a glove box, using a horizontal dilatometer (Adamel, Di22) under Ar atmosphere. The other experiments were performed in devices that were not in glove boxes.

XRD experiments were made in a classical θ-2θ diffractometer (Siemens, D500) with copper radiation, secondary graphite monochromator, scintillation detector. The lattice parameter was measured with an accuracy of $\pm 5.10^{-4}$ Å.

Table 1
Chemical analyses performed on Pu–Ce and Pu–Ga–Ce alloys. Impurity contents were lower than 30 wt. ppm for Ni, Fe, and Cr

Ce at.% (±0.3)	Ga at.% (±0.1)	
3.5	–	Under Ce stability limit
4.6	–	Ce stability limit
6.1	–	
8.1	–	
4.0	0.9	Ga stability limit
3.7	1.9	

EXAFS experiments were performed at LURE (beam DCI D44, Orsay, France) in a liquid nitrogen cryostat. Spectra were recorded in the transmission mode at the Pu L_{III}-edge (18053 eV), and in the fluorescence mode (with a 7-elements detector) at the Ce L_{III}-edge (5727 eV) and Ga K-edge (10367 eV). The interatomic distances are obtained with an accuracy of ± 0.01 Å. For both XRD and EXAFS measurements, the samples were confined in a plastic film allowing a good transparency to X-rays, and were placed in a sample holder.

The magnetic susceptibility device was studied by means of a Faraday balance equipped with a helium cryostat. Experiments were performed from room temperature down to 4 K (cooling rate of 1 K/min) at 0.8 and 1.4 Tesla. Samples were first sealed in a quartz tube (under He atmosphere), then placed in gold cylinders (to reduce the magnetic response from the sample holder), and finally enclosed in aluminum containers (under He atmosphere). The total susceptibility of the sample holder did not exceed 2.10^{-7} emu, and the susceptibility corrected from the sample holder contribution was given with an accuracy of $\pm 8.10^{-6}$ emu/mole.

For electrical resistivity measurements, a 500 μm thick sample (surface 2×5 mm^2) was electropolished and confined in a copper sample holder (under He atmosphere). Inside, the sample was maintained by four leads pressed on the sample; these ensured current flow and voltage pick-up. Experiments were performed from room temperature down to 4 K with a helium cryostat (1 K/min). The resistance was measured with an accuracy of ± 4 μΩ. The 4-points method unfortunately leads to a high incertitude in the determination of the resistivity ρ from the measured resistance R, mainly because of the small size of the sample, the size of the contacts, and the thin section approximation[2]. Thus, the normalized ρ/ρ_{295K} values were considered for quantitative comparison between different alloys.

3. Results

3.1. Thermal expansion

Thermal expansion of the four binary and two ternary alloys has been measured between 300 and 775 K. While the coefficient of thermal expansion α is always positive just above room temperature, it becomes negative at high temperature for low solute content, as for pure δ-Pu (δ-Pu being stable between 592 and 730 K). Fig. 1 displays the change in α with Ce content, together with previous results on Pu–Ga and Pu–Al alloys and pure δ-Pu metal in the temperature range where pure δ-Pu is stable and α essentially independent of temperature. Also shown is the α coefficient of the ternary PuCe3.7%Ga1.9% alloy. Pu–Ga and Pu–Al alloys follow the same trend whereas the change in α vs. solute content is different for Pu–Ce alloys. Results for low Ce contents show a strong dispersion that could be attributed to non monophased samples ($\alpha+\delta$ mixture) since the Ce content is close to the stability limit of the δ-phase.

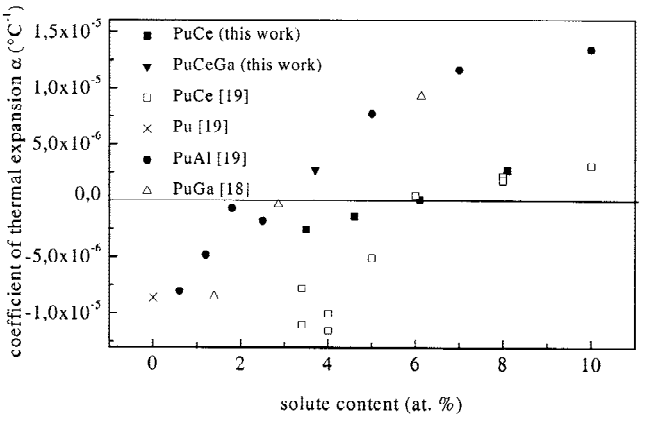

Fig. 1. Coefficient of thermal expansion α (taken between 592 and 730 K) vs. deltagen content for binary Pu–Ce ([19], this work), Pu–Ga [18] and Pu–Al [19] alloys, and ternary Pu–Ce3.7%–Ga1.9% alloy (this work), for which α is plotted vs. the sum of Ga and Ce contents.

3.2. XRD and EXAFS

The PuCe3.5% alloy with a Ce concentration below the reported stability limit has been found polyphased, containing some γ-phase. All the other alloys including PuCe4.6% at the stability limit and PuCe3.7%Ga1.9% where Ce content is below the stability limit are single phased. This last result already shows that stabilization effects by Ce and Ga are cooperative.

All XRD spectra exhibit similar narrow lines except for the richest in Ce, PuCe8.1% for which a broadening is clearly observable (Fig. 2).

The mean interatomic distance of the binary alloys increases gradually with the Ce content, as expected, but a discrepancy from Ellinger's results [20] is systematic. This cannot be explained by diffractometer calibration (carefully checked) nor chemical analysis errors as our measured concentrations give very good agreement with existing data for other physical properties. These results together with ternary XRD data and EXAFS data are reported in Fig. 3. EXAFS spectra obtained at the L_{III}-edge of Ce are of poor quality (low energy of the L_{III}-edge, influence of the Pu M-edges . . .); in that case, information was limited

[2]Relation between the resistance and the resistivity in the thin section approximation:

$$R=\rho\times\frac{1}{2e\pi}\ln\frac{(S_1+S)(S_2+S)}{S_1S_2}$$

where R is the resistance, ρ the resistivity, e the sample thickness and S_1,S_2, S the distances between the leads [17].

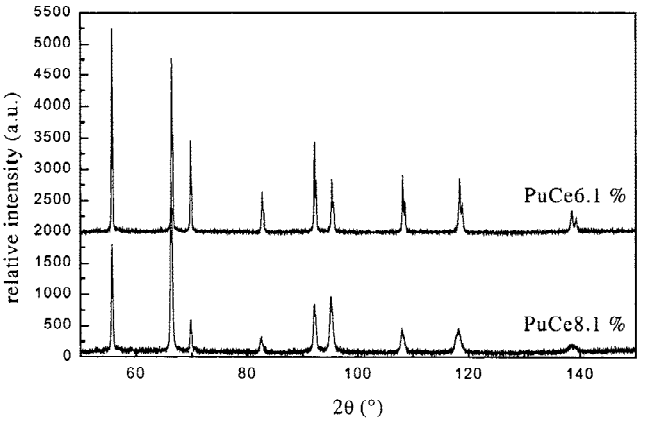

Fig. 2. XRD diagrams of the Pu–Ce8.1% and Pu–Ce6.1%, showing wider peaks for the PuCe8.1%.

to the first coordination shell and only two alloys were analyzed satisfactorily.

Surprisingly, Pu–Pu distances obtained by EXAFS are both smaller than those deduced from XRD and essentially constant at a 3.27 Å value, in agreement with recent results obtained by Villela et al. [21] on PuCe10%. This behavior is not observed in Pu–Ga alloys [10] and no explanation for this surprising result is found yet.

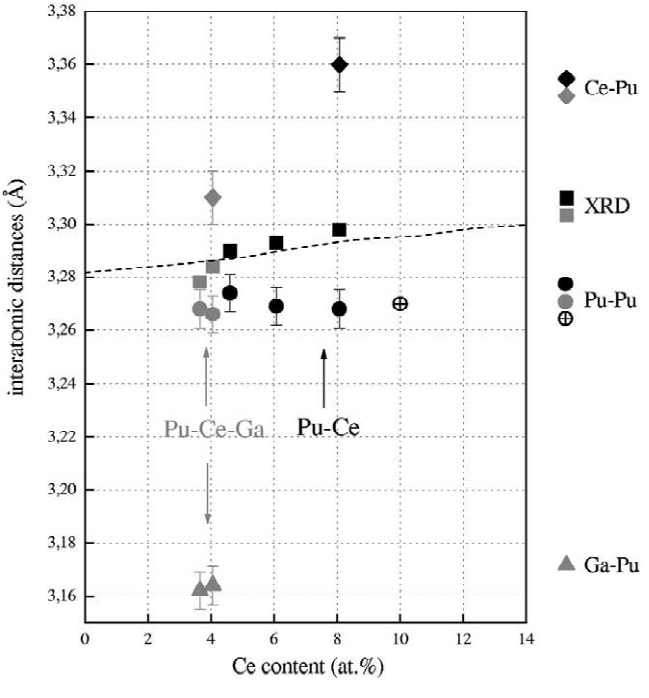

Fig. 3. Change in the first atomic distance around Pu, Ce and Ga atoms, measured by EXAFS. Black plots correspond to the Pu–Ce binary alloys and the gray plots correspond to the ternary Pu–Ce–Ga alloys. Empty circle enclosing a cross is extracted from Ref. [21] and the dashed line has been deduced from XRD measurements by Ref. [20].

3.3. Electrical resistivity

Electrical resistivity measurements on the six alloys together with literature data on Pu–Ga alloys are reported in Fig. 4 in which the martensitic transformation in PuCe4.6% is clearly visible. As it has been pointed out in Section 2, while our miniature four points apparatus allows to measure the resistance of small samples with arbitrary shape, it has the severe drawback to lead to a high uncertainty in the determination of the absolute resistivity. This prevents to compare the resistivity of different alloys as well as to compare our measurements with literature data.

Assuming that Matthiessen rule is followed, it is usual to write the electrical resistivity ρ as the sum of three contributions

$$\rho = \rho_0 + \rho_{\mathrm{ph}} + \rho_{\mathrm{mag}},$$

where ρ_0 is the residual resistivity due to impurities and defects, ρ_{ph} is the lattice resistivity due to scattering by phonons and ρ_{mag} is the magnetic resisitivity due to spin scattering. Apart from defects annealing, ρ_0 is constant, while ρ_{ph} is essentially linear above 20 K ($\theta_{\mathrm{D}}/10$, where θ_{D} is the Debye temperature). δ-Pu having the f.c.c. structure of thorium (Th), it is usual to assume similar contributions for ρ_0 and ρ_{ph} between δ-Pu, its alloys and Th [23]. Thus these terms represent no more than 10% of the total resistivity at room temperature and only 4% at 100 K: the magnetic contribution due to the 5f electrons represents most of the total resistivity. The abundant literature data on δ-Pu alloys show that $\rho(T)$ values converge quite well towards a common room temperature value following a large plateau above 150 K. This is in apparent contradiction with the Matthiessen rule except if the ρ_0 value is negligible compared to the $(\rho_{\mathrm{ph}}+\rho_{\mathrm{mag}})$ value. From the above consideration about thorium, this seems to be the case for δ-Pu alloys. This allows to use normalized values $\rho(T)/\rho(295\ \mathrm{K})$ for quantitative comparison between different alloys and also with literature data. As an example, Fig. 5 shows an excellent agreement between our results and Elliott's ones [17], while absolute values are very different.

Using this method it is also possible to extrapolate the normalized resistivity to 0 K and Fig. 6 shows $\rho(0\ \mathrm{K})/\rho(295\ \mathrm{K})$ vs. solute content for Pu–Ce, Pu–Ga and Pu–Al systems. The similar behavior for Pu–Ga and Pu–Al systems is consistent with the strong similarities between these two solutes as deltagen elements. The differences between Pu–Ce and Pu–Ga alloys suggests different electronic modification due to alloying. For the ternary alloys, both looking at them as adding Ce to Ga or Ga to Ce lead systematically to an increase in $\rho(0\ \mathrm{K})/\rho(295\ \mathrm{K})$.

For all the considered systems (Pu–Ga, Pu–Al, Pu–Ce) the normalized resistivity vs. solute content has been extrapolated to pure δ-Pu (0% solute content) at different temperatures. It is quite remarkable that these extrapolations lead to values that are independent of the nature of

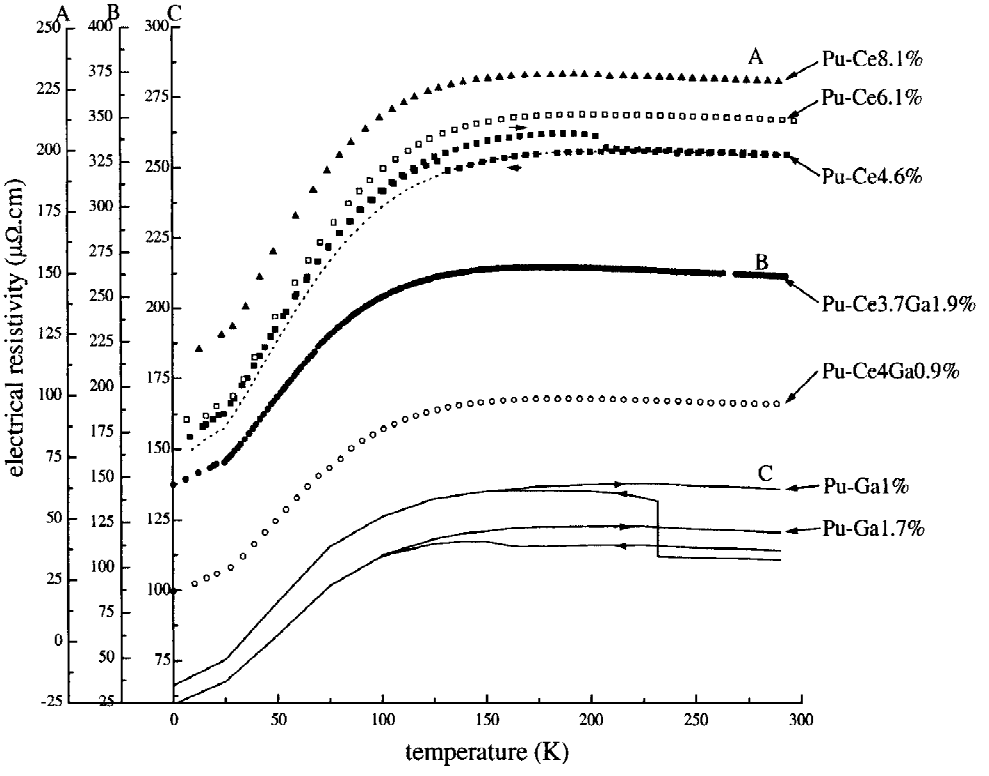

Fig. 4. Electrical resistivity change versus temperature, for binary Pu–Ce (this work) and Pu–Ga [22] alloys, and ternary Pu–Ce–Ga alloys (this work). A loss of electrical contact appeared at 50 K (decreasing temperature) for the Pu–Ce3.6% alloy; this was not restored during the temperature increase.

the solute within the accuracy of our measurements. It is then possible to represent the variation $\rho(T)$ of an hypothetical pure δ-Pu below the stability limit of this phase (592 K). Values are available only for temperature lower than 295 K since measurements have been performed between 295 and 4 K. This is displayed in Fig. 7 in which this curve seems to link up very well with the experimental one at the temperature of phase stability limit.

3.4. Magnetic susceptibility

True susceptibility values were obtained from the linear part of the magnetization M(H) after saturation of magnetic impurities. For all binary and ternary alloys, the susceptibility is essentially constant within the experimental accuracy which is about 1.5%. These results are reported in Fig. 8 together with previous results published on PuCe6%. No attempt to Curie–Weiss fit is possible on these flat $\chi(T)$ curves.

Thus, neither a temperature dependence nor a solute concentration dependence can be observed. This behavior is similar to that of Pu–Ga and Pu–Al alloys and no evidence of localization through Curie–Weiss behavior is obtained.

A much higher and temperature dependent susceptibility was obtained in Ref. [25] on Pu–Ce 6% alloys. However, it was noted that the alloy was not single phased. Our measurements show that this behavior must not be attributed to δ-PuCe6%.

The martensitic transformation observed in PuCe4.6% by electrical resistivity measurements is not detectable by magnetic susceptibility measurements. This is consistent with previous measurements on pure Pu between 4 and 600 K that showed almost the same susceptibility value for α-Pu and δ-Pu [26].

4. Discussion

4.1. Deltagen effects and crystal structure

The destabilization of the δ phase of Pu can be directly revealed by the presence, at room temperature and atmospheric pressure, of the α-phase, or by the occurrence at lower temperature of the martensitic transformation $\delta \rightarrow \alpha'$, α' being monoclinic α with solute atoms trapped in the lattice. Whereas PuCe3.5% is not monophased at room temperature (γ phase observed) all the other alloys, including the ternary alloys, are monophased with homogeneous grain size of about 40 μm as measured by

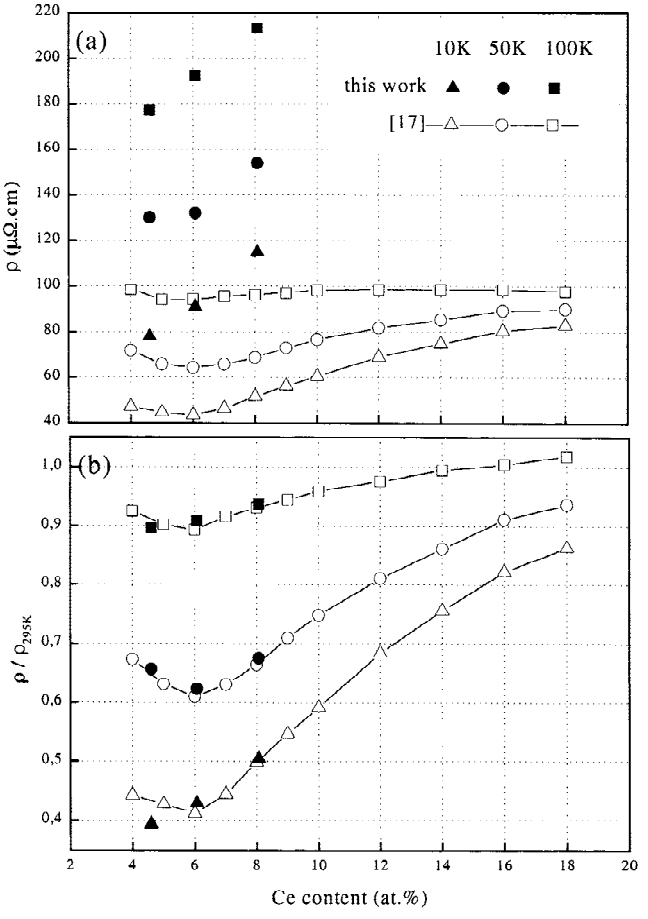

Fig. 5. Isotherms 10, 50 and 100 K of electrical resistivity (a) and normalized electrical resistivity (b). For the alloys exhibiting a martensitic transformation, the resistivity curve has been extrapolated below the martensitic transformation temperature, with the assumption that the α phase occurrence induces only a translation of the curve (corresponding to the observed step) [17].

micrography. The coefficient of thermal expansion α including ternary alloys is higher than the one for the corresponding PuGa or PuCe binary alloys (Fig. 1); this

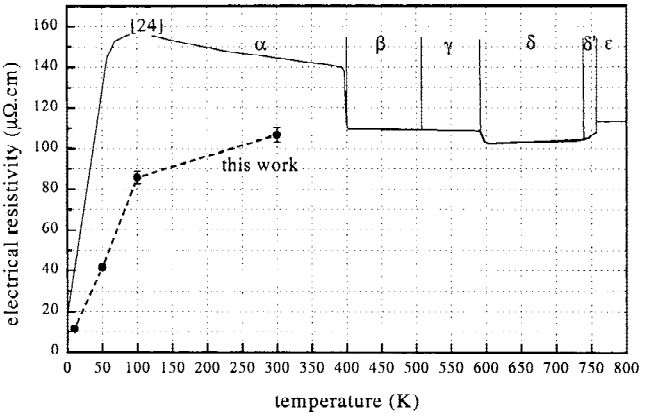

Fig. 7. Electrical resistivity of the δ phase extrapolated to low temperature and compared with electrical resistivity of pure Pu [24].

suggests that the deltagen effects of Ce and Ga are not antagonist. At low temperature δ-PuCe4.6% transforms to α′ (martensitic start temperature: 140 K). There is no evidence of martensitic transformation in the other alloys including the ternary alloys which confirms the additive deltagen effects of Ce and Ga.

An important result concerns the Pu–Pu distances (obtained by EXAFS); the Pu–Pu distances are indeed about 6% smaller than the mean distance obtained by XRD. This difference is definitely outside experimental errors and has a physical origin, being observed on several different alloys, using different synchrotron sources and models for analysis. While we do not have yet a satisfying explanation for this apparent contradiction, the unique behavior of Ce that can adapt its atomic volume (see next paragraph) may be at the origin of this result. The X-ray diffraction lines broadening observed for the Pu–Ce8.1% can not be attributed to a change in grain size which remains constant whatever the Ce content. It is tempting to draw a correlation between these results and the dipersion in Pu–Pu and Ce–Pu distances observed by EXAFS.

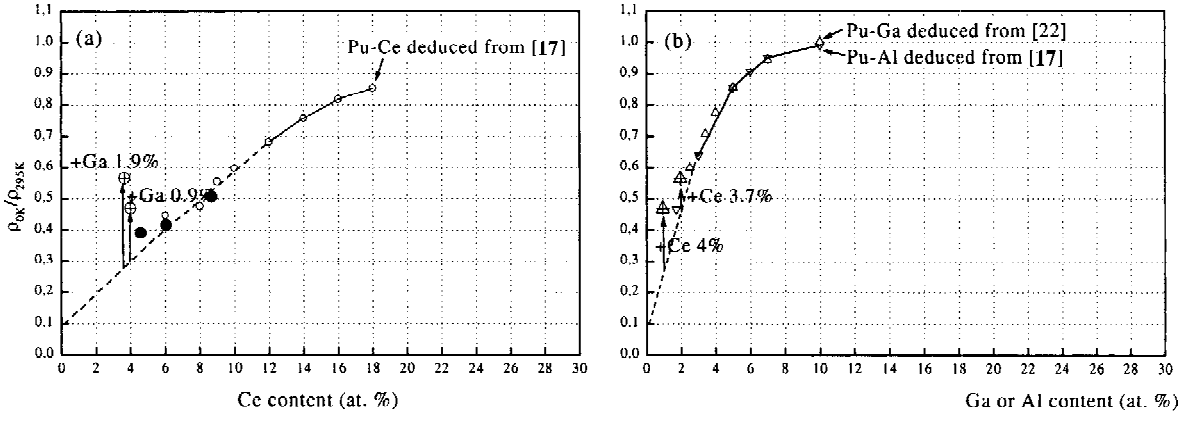

Fig. 6. Change in ρ_{0K}/ρ_{295K} vs. Ce content (a) and Ga/Al content (b) for binary Pu–Ce ([17], this work), Pu–Ga [22], Pu–Al [17] alloys, and ternary Pu–Ce–Ga alloys (this work).

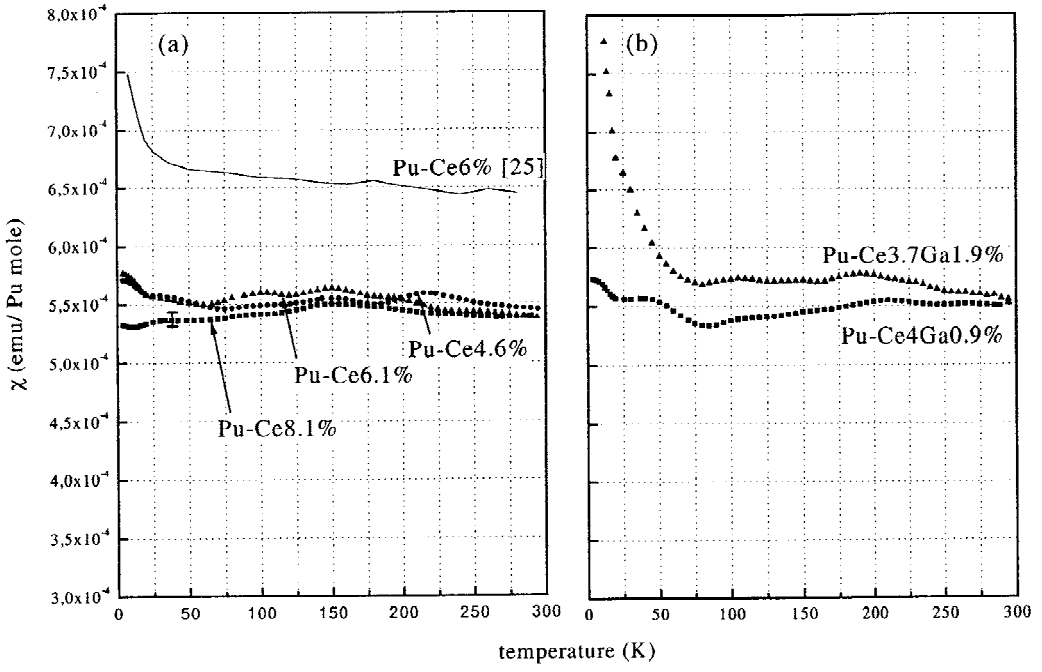

Fig. 8. Change in the magnetic susceptibility vs. temperature for binary Pu–Ce ([25], this work) (a), and ternary Pu–Ce–Ga alloys (this work) (b). The signal increase observed under 70 K for the Pu–Ce3.7Ga1.9% is thought to be due to the presence of a foreign phase in the sample.

4.2. Electronic structure

As recalled in the introduction, not only Pu but also Ce are extraordinary metals. They both have f electron states at the threshold of localization. They both show allotropic transformation involving huge volume changes (21% increase for the $\alpha-\gamma$ transition in Ce, 24% increase for the $\alpha-\delta$ transition in Pu), which can be driven by temperature or by pressure.

In both cases this huge volume change has been related to a localization process of the f states: is this process exactly the same for Ce and Pu? A comparative discussion is of some interest here for a better understanding of the Pu–Ce alloys.

The expanded γ-Ce phase is clearly trivalent like a normal rare earth [27]: the one 4f electron state is atomic-like which is confirmed by the physical properties of γ-Ce starting with its atomic volume and its magnetic susceptibility. But as recalled in the Introduction this is not yet the case of expanded δ-Pu and we can also say this is confirmed by its atomic volume and its magnetic susceptibility. If there is an overall agreement about a localization step between α-Pu and δ-Pu, the precise behavior of the 5f states in δ-Pu is still a subject of research and debate: they are strongly correlated but what is the exact nature of these correlated states?

We have proposed a Kondo-type intraatomic correlation between local 5f states and band states [25]: this was based on the log T dependence of the electrical resistivity at high temperature in all stabilized δ-Pu alloys and recent results on irradiation effects in δ stabilized Pu alloys favor this approach [28]. Other models have also been proposed, all trying to reconcile essentially localized 5f states with a temperature independent susceptibility and a very large resistivity.

At the other end, while it is now generally agreed that 5f states in α-Pu are band states, the case of α-Ce is controversial: after the failure of the promotional model, inconsistent with photoemission results [29], Johansson [30] explained the $\gamma-\alpha$ transition as a Mott transition within the 4f electron shell, the 4f states becoming band states in α-Ce. A Kondo Volume Collapse model was also proposed [31]. Calculations including combined SIC-LDA (Local-Density-Approximation) and Anderson impurity model [32] describe correctly some experimental results. Thus, it appears that the electronic structure of α-Ce remains an open problem.

Table 2 summarizes this by sorting Pu, Ce and Am comparing their f electronic feature.

A striking singularity is observed in the f.c.c. Pu–Ce solid solution, making it quite unusual and spectacular, as shown on Fig. 9 where the lattice parameter is plotted versus the Ce content for stable [20] and metastable [15] Pu–Ce alloys. Above 75% Ce, the Vegard's law is well followed between δ-Pu and γ-Ce. At 75% Ce, a drastic decrease in the lattice parameter occurs (3.8%) which means that the Vegard's law between δ-Pu and γ-Ce is not followed any more for lower Ce contents. Starting from low Ce contents, Ellinger [20] extrapolated his experimental results to 4.84 Å at 100% Ce: this parameter corresponds to α-Ce under 1.5 GPa [19] while a lattice of 4.96 Å can be deduced for α-Ce at ambient pressure, using the law

Table 2
Electronic features of Pu, Ce and Am

Narrow 4f/5f bands	Intermediate valent system	Localized 4f/5f electrons
α-Pu	δ-Pu	α,β-Am
α′-Ce (pressure>4 GPa)	α-Ce ?	γ-Ce
α-Ce ?		

describing the Ce volume vs. pressure up to 10 GPa [33]. Therefore, a second predicted lattice parameter evolution (with respect to the Vegard's law) is considered between δ-Pu and α-Ce. From it, a negative deviation occurs for both Ellinger's results (stable solid solutions) and Giessen's results [15] (metastable solid solutions).

Vegard's law being the signature of a pure steric behavior, deviations from it must be interpreted in terms of electronic effects. In the case of Pu–Ce alloys, both 4f and 5f electrons are facing the localization process: any f localization leads to an increase in the volume of the corresponding atom. Then, both 4f electrons delocalization in Ce (α-Ce or, as shown in the Th–Ce system, γ-Ce [34]), which is due to the small δ-Pu lattice, and 5f electrons localization in Pu, due to large Ce atoms, must contribute. Above 75 at.%Ce, a plot of the deviation with respect to the Vegard's law between δ-Pu and γ-Ce shows a positive deviation for δ-Pu–γ-Ce alloys, as observed in the δ-Pu–Am system (Fig. 10). 4f electrons being quite localized in γ-Ce, the deviation is associated with a preponderant localization of the 5f electrons in δ-Pu. On the opposite, below 70 at.%Ce, the observed deviation from Vegard's law (between δ-Pu and α-Ce) is negative, suggesting that the 4f(Ce) delocalization must be preponderant. At 70 at.%Ce, the lattice stress due to the small Pu atoms corresponds to the pressure inducing the γ to α transition in pure Ce.

EXAFS measurements show a larger Ce–Pu distance than Pu–Pu distance, which confirms the steric effect of Ce. Nevertheless, the Pu–Pu distances do change with Ce content whereas the lattice parameter increases. Moreover, Pu–Pu distances deduced from EXAFS are significantly different from those deduced from X-ray diffraction.

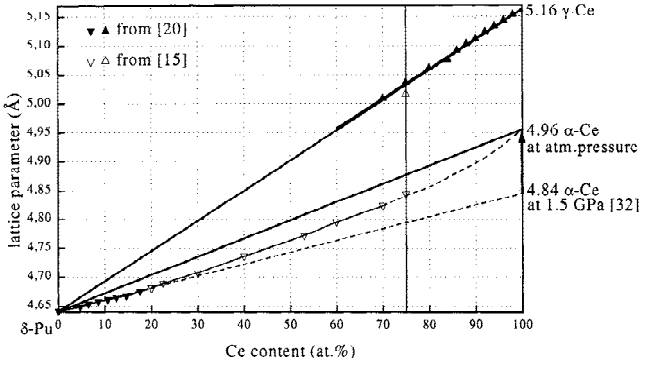

Fig. 9. Change in the lattice parameter of Pu–Ce alloys vs. Ce content.

In Pu–Ga alloys, the Pu–Pu distances deduced from both EXAFS and XRD measurements are, on the contrary of Pu–Ce alloys, the same [10] and change with gallium concentration.

The discrepancy between Pu–Pu distances deduced from EXAFS and XRD measurements could be attributed to the averaging nature of the XRD measurements which are global while EXAFS are local ones. XRD distances could then be seen as a weighted average between Pu–Pu and Ce–Pu distances. This is consistent with the broadening of the XRD peaks observed in the PuCe8.1% alloy. It would be interesting to have the Pu–Pu, Ce–Pu distances and XRD results for higher cerium contents. In the case of Pu–Ga alloys, the light gallium atoms barely contribute to the X-ray scattering compared to the heavy plutonium atoms. Nevertheless, it would be interesting to study more in detail the width of the XRD peaks as a function of gallium content.

Regarding the constant Pu–Pu interatomic distances observed for the Pu–Ce(–Ga) alloys, it suggests a weak effect of cerium on the localization of the 5f electrons states: this is consistent with the very similar magnetic susceptibility curves obtained.

Despite this apparent weak effect of Ce on the electronic structure of Pu, this solute is not inert. Indeed, Ce addition in a Pu–Ga1% alloy makes the martensitic transformation disappear and leads to an increase in the δ phase expansion coefficient: this demonstrates that Ga and Ce have an additive effect regarding the δ phase stability.

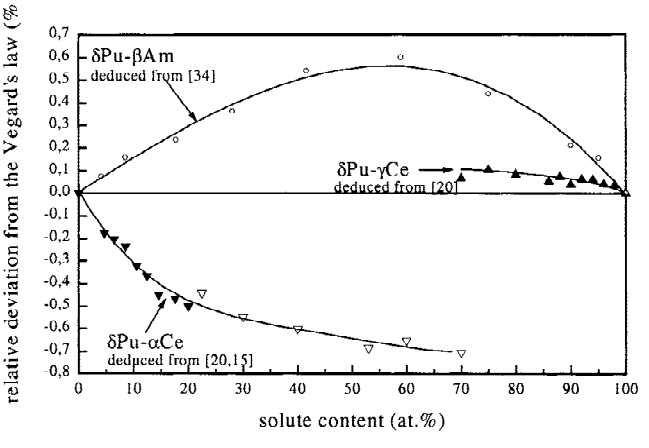

Fig. 10. Change in the relative deviation from the Vegard's law vs. solute content (lines are guides for the eyes).

5. Conclusion

Understanding the effect of Ce upon the behavior of the 5f electron states in δ stabilized Pu–Ce(–Ga) solid solutions requires to know the precise organization of the atoms in the f.c.c. lattice, both at long and short range.

It appears that for low concentrations, Ce is α-like, while for high concentrations (above 75%) it is γ-like: the smaller size of Pu atoms induces an internal pressure which induces a γ–α transition in Ce as Pu is added to it. For low Ce concentrations α-like Ce atoms appear quite soft and adapt their size to the requirements of Pu atoms. This rather unique behavior may be at the origin of the discrepancy between local and mean values of the Pu–Pu distances, leading also to a weaker localization process of the 5f electrons than expected due to the increase in the lattice parameter with increased Ce content in the solid solution. Investigating other alloys with higher Ce content is necessary to get more information about the crystalline structure and about a possible sign of clear 5f localization. Moreover the high temperature expansion coefficient has been obtained for all δ stabilized Pu alloys as a function of concentration. This may be useful in better understanding the still unexplained negative thermal expansion of δ-Pu.

The very important magnetic diffusion term in the electrical resistivity allows the use of normalized resistivity curves for the comparison of the different δ-stabilized Pu alloys. The analysis then allows to obtain a full resistivity curve for δ-Pu down to 0 K although δ-Pu is not stable below 592 K.

In ternary Pu–Ce–Ga alloys, the additive deltagen effects of Ce and Ga has been demonstrated.

Acknowledgements

We would like to express our appreciation to Professor J.C. Niepce for helpful suggestions and discussions. We also wish to thank Mrs V. Briois and Mrs S. Belin from LURE for helping with the EXAFS measurements.

References

[1] J. Bouchet, B. Siberchicot, F. Jollet, A. Pasturel, J. Phys. Condens. Matter 12 (2000) 1723.
[2] S.Y. Savrasov, G. Kotliar, E. Abrahams, Nature 410 (2001) 793.
[3] F.H. Ellinger, K.A. Johnson, C.C. Land, Los Alamos Scientific Laboratory, unpublished work as of June, 1967.
[4] V.I. Kutaitsev, N.T. Chebotarev, I.G. Lebedev, M.A. Andrianov, V.N. Konev, T.S. Menshikova, Plutonium 1965, Proceedings of the third International Conference on Plutonium, London, 1965, in: A.E. Kay, M.B. Waldron (Eds.), United Kingdom Atomic Energy Authority, London, Chapman and Hall for the Institute of Metals (Eds.), 1967, p. 420.
[5] L. Pauling, J. Am. Chem. Soc. 69 (1947) 542.
[6] W.H. Zachariasen, J. Inorg. Nucl. Chem. 35 (1973) 3487.
[7] A.W. Lawson, T.Y. Tang, Phys. Rev. 76 (1949) 301.
[8] F.H. Ellinger, C.C. Land, V.O. Struebing, J. Nucl. Mat. 12 (2) (1964) 226.
[9] F.H. Ellinger, C.C. Land, W.N. Miner, J. Nucl. Mat. 5 (2) (1962) 165.
[10] Ph. Faure, B. Deslandes, D. Bazin, C. Tailland, R. Doukhan, J.M. Fournier, A. Falanga, J. Alloys Comp. 244 (1996) 131.
[11] L.E. Cox, R. Martinez, J.H. Nickel, S.D. Conradson, P.G. Allen, Phys. Rev. B 51 (1995) 751.
[12] P. Weinberger, A.M. Boring, J.L. Smith, Phys. Rev. B 31 (1985) 1964.
[13] A.M. Boring, J.L. Smith, Challenges in Plutonium Science, volume I, Los Alamos Science 26, in: N.G. Cooper (Ed.), Los Alamos National Laboratory, 90 (2000).
[14] B.R. Cooper, Challenges in Plutonium Science, volume I, Los Alamos Science 26, in: N.G. Cooper (Ed.), Los Alamos National Laboratory, 154 (2000).
[15] B.C. Giessen, V.O. Struebing, R.O. Elliott, Mat. Sci. Eng. 18 (1975) 239.
[16] T. Gouder, private communication.
[17] R.O. Elliott, C.E. Olsen, J. Louie, J. Phys. Chem. Solids 23 (1962) 1029.
[18] M. Taylor, J. Nucl. Mat. 31 (1969) 339.
[19] W.N. Miner, F.W. Schonfeld, Plutonium Handbook, in: O.J. Wick (Ed.), Pacific Northwest Laboratories, The American Nuclear Society, La Grange Park, Illinois, USA (1967).
[20] F.H. Ellinger, C.C. Land, E.M. Cramer, in: W.D. Wilkinson (Ed.), Extractive and Physical Metallurgy of Plutonium and its Alloys, Vol. 149, Interscience Publishers, New York, 1960.
[21] P. Villela, F.J. Espinosa-Faller, J.C. Lashley, S.D. Conradson, L.E. Cox, B. Martinez, R. Martinez, R. Pereyra, J. Terry, L. Morales, Phys. Rev. B, to be published.
[22] J. Joel, C. Roux, M. Rapin, J. Nucl. Mat. 40 (1971) 297.
[23] D.T. Peterson, D.F. Page, R.B. Rump, D.K. Finnemore, Phys. Rev. B 153 (3) (1967) 701.
[24] R.B. Gibney, T.A. Sandenaw, internal report from Los Alamos, n° 1883 (1967).
[25] S. Méot-Reymond, J.M. Fournier, J. Alloys Comp. 232 (1996) 119.
[26] N. Buclet, J.M. Fournier, M. Dormeval, L. Jolly, F. Wastin, E. Colineau, J. Rebizant, G. Lander, 2nd workshop on Orbital and Spin Magnetism of Actinides, Berkeley, October, 2002.
[27] A. Svane, Phys. Rev. B 53 (8) (1996) 4275.
[28] M. Fluss, to be published.
[29] D.M. Wieliczka, C.G. Olson, D.W. Lynch, Phys. Rev. B 29 (1984) 2028.
[30] B. Johansson, Philos. Mag. 30 (1974) 469.
[31] J.W. Allen, R.M. Martin, Phys. Rev. Lett. 49 (1982) 1106;
R.M. Martin, J.W. Allen, J. Magn. Mater. 47&48 (1985) 257.
[32] J. Lægsgaard, A. Svane, Phys. Rev. B 59 (5) (1999) 3450.
[33] K.A. Gschneidner Jr., Rare Earth Alloys, D. Van Nostrand Company, Princetown, NJ, 1961.
[34] J.H.N. van Vucht, Philips Res. Rep. 12 (1957) 351;
R.T. Weiner, W.E. Freeth, G.V. Raynor, J. Inst. Metals 86 (1957–1958) 185;
D.S. Evans, G.V. Raynor, J. Nucl. Mat. 5 (3) (1962) 308.